International Journal of the Korean Society of Precision Engineering Vol. 4, No. 2, March 2003.

A Study on the Sensorless PMSM Control using the Superposition Theory

Young-Jin Lee[1], Young-Jin Yoon[2], Young-Ho Kim[3] and Man-Hyung Lee[4]

[1] Research Institute of Computer Information and Communication, Pusan National University, Pusan, South Korea
[2] Department of Mechanical and Intelligent Systems Engineering, Pusan National University, Pusan, South Korea
[3] Division of Electrical and Computer Engineering, Pusan National University, Pusan, South Korea
[4] School of Mechanical Engineering, Pusan National University, Pusan, South Korea

ABSTRACT

This study presents a solution to control a PMSM without sensors. The control method is the presented superposition principle. This method of sensorless theory is very simple to compute estimated angle. Therefore, computing time to estimate angle is shorter than other sensorless methods. The use of this system yields enhanced operations, fewer system components, lower system costs, efficient energy control system designs and increased efficiencies. A practical solution is described and its results are given in this study. The performance of a sensorless architecture allows an intelligent approach to reduce the complete system costs of digital motion control applications using the cheaper electrical sensorless motors. This paper deals with an overview of solutions in the sensorless PMSM control applications, whereby the focus will be the new sensorless controller and its applications.

Keywords : PMSM, Sensorless Control, Superposition Theory

1. Introduction

By the extension of modern automated equipments, the use of servomotor in the industrial and household machines has been on the rapid rise, and the servomotor has been used for the indispensable source of drive in every industrial fields from the industrial robot and all sorts of numerical control machine tools to the household machines.

In a few years ago, most servomotors meant to be DC servomotor using ferrite permanent magnet but they have several weaknesses about frequent inspection and repair and also some problems on high speed operation by reason of brush and commutator. However, AC servomotor using permanent magnet has more complicated control scheme than that of DC servomotor, but has big advantages over both durability and large ratio of power per weight and torque per current because it deals the rectification of DC motor with electrical switching. Recently, high- performance AC motors have been more often used, together with the developments of control technology, semiconductor element and microprocessor. Among them, a permanent magnet synchronizing motor has been generally used in the industrial world. Hereafter, we call it PMSM. It has a disadvantage that properly handled switching is needed to drive AC servomotor and then position detecting device is also necessary to obtain information on the rotor's position angle. An encoder and a resolver are generally used to detect rotor's position angle, but these exterior mechanical position sensor has not only an economic disadvantage also problem on reliability by sensor's sudden characteristic change in the worse circumstances. In this case, PMSM has an absolute disadvantage over the machinery used in crash worthiness, corrosion resistance, high temperature, and high humidity. There have been vigorous studies on a

sensorless drive for low cost of sensor installation and good robustness on exterior environment.

There are a lot of papers about sensorless control method of motor[1-6]. It can be largely divided by back EMF estimation method, magnetic flux estimation method, and state observer method. Back EMF estimation method is to measure voltage and current, and then directly calculate back EMF from stator's voltage equation. But because this method differentiates current, there are possibility to increase noise. To overcome this problem, we can use filter. But phase delay problem is still remain. Especially because there is no back EMF in the initial state of motor, it is impossible to get the position of motor. Magnetic flux estimation method is to get magnetic flux from measurement value of voltage and current. Because this method uses integration in order to get the magnetic flux, it occurs integrator drift effect. Therefore we needs calibration method. Algorithms like sliding mode observer, extended kalman filter, and so on are introduced in the state observer method. the method has merits like position and velocity compensation, and initial driving. But the algorithm is complicate, and needs high speed operational controller like DSP, to accomplish real time control. Though this method is reported as paper with experimental result, which depends upon performance of processor.

In this paper, a sensorless control algorithm is proposed to overcome a disadvantage of system using the position sensor. Moreover, its basic theory is based on the superposition principle. That is, motor's state equation is divided into two conditions for analysis: one is the state equation of exciting voltage and phase current in a constraint, the other is the state equation of back EMF (Electromotive Force) and phase current in a short circuit. Based on these analyses, we proposed the new method that it computed simply short circuit current by motor's back EMF in operation and then obtained the information on position angle. It is also proved that the proposed method is presented to be proper by simulation and experimental results.

2. The Modelling of the PMSM

2.1 The Voltage Equation of Motor

The equivalent circuit to analyse numerically 3-phase PMSM with sinusoidal distribution of back EMF is shown in Fig. 1. The voltage, current, and impedance equations obtained from this equivalent circuit, that is, the circuit equations are represented as Equation 1.

$$\begin{bmatrix} v_a \\ v_b \\ v_c \end{bmatrix} = \begin{bmatrix} R_a & 0 & 0 \\ 0 & R_b & 0 \\ 0 & 0 & R_c \end{bmatrix} \begin{bmatrix} i_a \\ i_b \\ i_c \end{bmatrix} + \frac{d}{dt} \left\{ \begin{bmatrix} L_{aa} & M_{ab} & M_{ac} \\ M_{ba} & L_{bb} & M_{bc} \\ M_{ca} & M_{cb} & L_{cc} \end{bmatrix} \begin{bmatrix} i_a \\ i_b \\ i_c \end{bmatrix} \right\} + \begin{bmatrix} e_a \\ e_b \\ e_c \end{bmatrix} \quad (1)$$

, where v_a, v_b and v_c are motor's phase voltages at a, b, c, i_a, i_b and i_c are phase currents at a, b, c, e_a, e_b and e_c are back EMFs induced from phase stator coil at a, b, c, R_a, R_b and R_c are the coil resistances at each phase, L_{aa}, L_{bb} and L_{cc} are magnetic inductances at each phase, $M_{ab}, M_{ac}, M_{bc}, M_{ba}$, M_{ca} and M_{cb} are mutual inductances between each coil, respectively. The stator coil of PMSM with sinusoidal back EMF as Fig. 1 has the symmetric structure at 120°in the same coils and each flux occurred at a phase intercrosses at a half for other phases. In representing motor's cylindrical rotator characteristic, each stator's magnetic inductance depends on the combination of leakage flux and the intercrossing flux shares stator' phases equally.

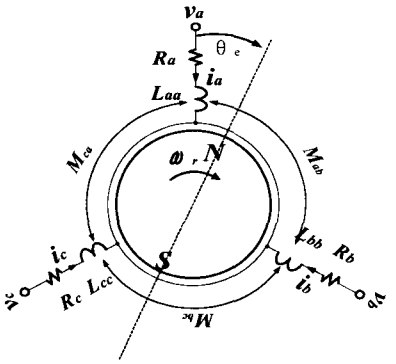

Fig. 1 Three Phase Equivalent circuit of PMSM

In addition, this magnetic inductance can be regarded as rotor's position and independent variable. Therefore, each phase has an equal armature coil resistance and armature coil resistances R_a, R_b and R_c can be replaced with R, and mutual inductances between armature coils $M_{ab}, M_{ac}, M_{bc}, M_{ba}$, M_{ca} and M_{cb} can be replaced with $-\frac{1}{2}M$, self inductances L_{aa}, L_{bb} and L_{cc} can be replaced with L_a.

The voltage equations of Equation 1 in motor variables obtained from the above can be represented as follows.

$$\begin{bmatrix} v_a \\ v_b \\ v_c \end{bmatrix} = \begin{bmatrix} R+pL_a & -p\frac{M}{2} & -p\frac{M}{2} \\ -p\frac{M}{2} & R+pL_a & -p\frac{M}{2} \\ -p\frac{M}{2} & -p\frac{M}{2} & R+pL_a \end{bmatrix} \begin{bmatrix} i_a \\ i_b \\ i_c \end{bmatrix} + \begin{bmatrix} e_a \\ e_b \\ e_c \end{bmatrix} \quad (2)$$

, where p is a differentiator ($p = \frac{d}{dt}$).
The stator's magnetic inductance is following the next equation

$$L_a = l + M \quad (3)$$

, where l represents a motor's leakage inductance. If the motor is connected in the Y form, 3-phase current becomes parallel and then it can be represented as Equation 4.

$$i_a + i_b + i_c = 0 \quad (4)$$

The voltage equation of PMSM from Equation 2,3, and 4 can be shown into simple 3×3 matrix form.

$$\begin{bmatrix} v_a \\ v_b \\ v_c \end{bmatrix} = \begin{bmatrix} R+pL & 0 & 0 \\ 0 & R+pL & 0 \\ 0 & 0 & R+pL \end{bmatrix} \begin{bmatrix} i_a \\ i_b \\ i_c \end{bmatrix} + \begin{bmatrix} e_a \\ e_b \\ e_c \end{bmatrix} \quad (5)$$

, where $L = l + \frac{3}{2}M$.
each inductive EMF of Equation 5, e_a, e_b and e_c are represented as each differentiator of flux intercrossed at phase coils. So, let the maximum value of intercrossing flux $\lambda_a \lambda_b$ and λ_c at phase a, b, and c be λ_m, each representation can be as follows.

$$\begin{aligned} \lambda_a &= \lambda_m \cos(\theta_e) \\ \lambda_b &= \lambda_m \cos(\theta_e - \tfrac{2}{3}\pi) \\ \lambda_c &= \lambda_m \cos(\theta_e + \tfrac{2}{3}\pi) \end{aligned} \quad (6)$$

, where θ_e is a clockwise electrical rotor angle with reference to the stator coil at phase a. The inductive EMF obtained from intercrossing flux of phase coil is represented into Equation 7.

$$\begin{aligned} e_a &= \frac{d}{dt}\lambda_a = -\omega_e \lambda_m \sin(\theta_e) \\ e_b &= \frac{d}{dt}\lambda_b = -\omega_e \lambda_m \sin(\theta_e - \tfrac{2}{3}\pi) \\ e_c &= \frac{d}{dt}\lambda_c = -\omega_e \lambda_m \sin(\theta_e + \tfrac{2}{3}\pi) \end{aligned} \quad (7)$$

, where ω_e means an rotor's angular velocity and is given as follows.

$$\omega_e = \frac{d}{dt}\theta_e \quad (8)$$

2.2 The Coordinates Transformation of 3- Phase AC Circuit Equation

It is more convenient to represent 2-phase AC than 3-phase in the voltage and current for understanding of 3-phase PMSM characteristic and derivation of control method Like the above, the coordinates need to be transformed for different analysis on motor, and it is called to the coordinates transformation. The transformation matrix from 3-phase AC coordinates (a-b-c) to 2-phase AC coordinates(α-β) can be defined as Equation 9 and this transformation results in the motor's equivalent circuit in the fixed 2 axis α-β coordinates at Fig. 2.

$$C = \sqrt{\frac{2}{3}} \begin{bmatrix} 1 & -\frac{1}{2} & -\frac{1}{2} \\ 0 & \frac{\sqrt{3}}{2} & -\frac{\sqrt{3}}{2} \end{bmatrix} \quad (9)$$

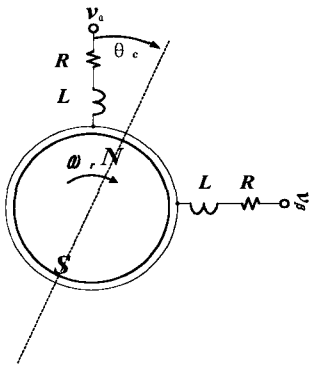

Fig. 2 Two Phase Equivalent circuit of PMSM

The voltage equation of 2-phase equivalent circuit of PMSM in the fixed coordinates is given into Equation 10.

$$\begin{bmatrix} v_\alpha \\ v_\beta \end{bmatrix} = \begin{bmatrix} R+pL & 0 \\ 0 & R+pL \end{bmatrix} \begin{bmatrix} i_\alpha \\ i_\beta \end{bmatrix} + \begin{bmatrix} e_\alpha \\ e_\beta \end{bmatrix} \quad (10)$$

This equation can be obtained by multiply the transformation matrix C and the given 3-phase circuit equation together in Equation 5.

, where v_α, v_β, i_α, i_β, e_α and e_β are given as follows, respectively.

$$\begin{aligned} v_\alpha &= \sqrt{\frac{2}{3}}\left(v_a - \frac{v_b}{2} - \frac{v_c}{2}\right) \\ v_\beta &= \frac{(v_b - v_c)}{\sqrt{2}} \end{aligned} \quad (11)$$

$$\begin{aligned} i_\alpha &= \sqrt{\frac{2}{3}}\left(i_a - \frac{i_b}{2} - \frac{i_c}{2}\right) \\ i_\beta &= \frac{(i_b - i_c)}{\sqrt{2}} \end{aligned} \quad (12)$$

$$\begin{aligned} e_\alpha &= -\sqrt{\frac{3}{2}}\,\omega_e \lambda_m \sin(\theta_e) \\ e_\beta &= \sqrt{\frac{3}{2}}\,\omega_e \lambda_m \cos(\theta_e) \end{aligned} \quad (13)$$

If the Equation 10 obtained from the 2-axis fixed coordinates(α-β) is rearranged and also represented into the state equation of PMSM, the Equation 14 can be given as follows

$$\begin{bmatrix} i_\alpha \\ i_\beta \end{bmatrix} = \begin{bmatrix} -\frac{R}{L} & 0 \\ 0 & -\frac{R}{L} \end{bmatrix} \begin{bmatrix} i_\alpha \\ i_\beta \end{bmatrix} + \frac{1}{L}\begin{bmatrix} v_\alpha \\ v_\beta \end{bmatrix} - \frac{1}{L}\begin{bmatrix} e_\alpha \\ e_\beta \end{bmatrix} \quad (14)$$

, where the torque equation is given into Equation 15.

$$T_e = p_{poles} \cdot \lambda_m(-i_\alpha \sin\delta + i_\beta \cos\delta) \quad (15)$$

, where δ stands for the angle between rotor and stator.

2.3 The Principle of Sensorless PMSM using Superposition Principle

The voltage equation of PMSM given in 2-phase AC coordinates α-β can be represented into the equivalent circuit in the 2 fixed reference axis(α-β) in Fig. 3 and from Equation 10.

As you can see in the circuit of α-βcoordinates in Fig. 3, the sources forming the motor current are a back EMF voltage and a terminal voltage as two voltage sources. Accordingly, the use of superposition principle which separates into two voltage source can be represented into the equivalent circuit in Fig. 4.

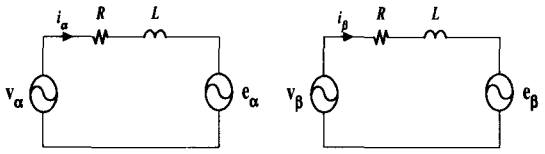

(a) Equivalent circuit of α axis (b) β axis

Fig. 3 Equivalent circuit of PMSM by α-β axis

According to Fig. 4, the source of current through motor can be expressed the inductive EMF term occurred by the phase voltage from inverter and the motor's rotation. The motor current becomes a indispensable factor for overcurrent detection and excellent velocity control of motor. If the motor parameters R and L can be known, the current component by the phase voltage induced from inverter can be found easily. In the equivalent circuit of Fig. 4, the circuit represented with the inductive EMF by the motor's rotation and the phase voltage from inverter can be obtained into the following state equation.

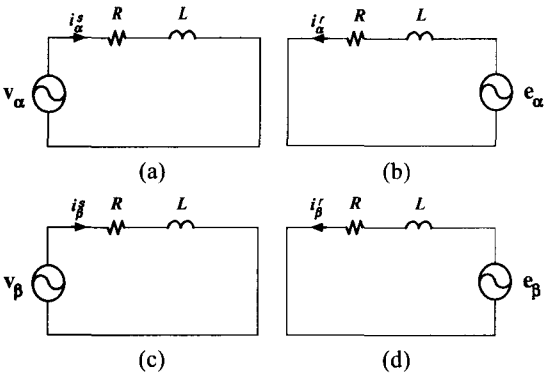

Fig. 4 Equivalent circuit of PMSM using superposition principle

(a) Equivalent circuit of α axis terminal voltage
(b) Equivalent circuit of α axis back EMF voltage
(c) Equivalent circuit of β axis terminal voltage
(d) Equivalent circuit of β axis back EMF voltage

$$\begin{bmatrix} i^s_\alpha \\ i^s_\beta \end{bmatrix} = \begin{bmatrix} -\frac{R}{L} & 0 \\ 0 & -\frac{R}{L} \end{bmatrix} \begin{bmatrix} i^s_\alpha \\ i^s_\beta \end{bmatrix} + \frac{1}{L}\begin{bmatrix} v_\alpha \\ v_\beta \end{bmatrix} \quad (16)$$

$$\begin{bmatrix} i^r_\alpha \\ i^r_\beta \end{bmatrix} = \begin{bmatrix} -\frac{R}{L} & 0 \\ 0 & -\frac{R}{L} \end{bmatrix} \begin{bmatrix} i^r_\alpha \\ i^r_\beta \end{bmatrix} - \frac{1}{L}\begin{bmatrix} e_\alpha \\ e_\beta \end{bmatrix} \quad (17)$$

The current term by the back EMF can be computed by the difference between the detected real motor current and the current by the phase voltage. Therefore, the current component can be easily obtained, and then this current component of back EMF comes to be directly controlled by the voltage of back EMF.

$$i^r{}_a(t) = \frac{e_a(t)}{R}(1-e^{-\frac{R}{L}t}) + i^r{}_a(0)\, e^{-\frac{R}{L}t} \tag{18}$$

This solution can be represented into the discrete form as Equation 19.

$$i^r{}_a(n) \fallingdotseq \frac{e_a(n)}{R}(1-e^{-\frac{R}{L}\triangle T}) + i^r{}_a(n-1)\, e^{-\frac{R}{L}\triangle T} \tag{19}$$

If motor parameter and sampling time are determined, the exponential term of Equation 19 can be dealt with the constant, and its value can be defined as follows.

$$K_T \fallingdotseq e^{-\frac{R}{L}\triangle T} \tag{20}$$

Thus, the back EMF term from Equation 19 and 20 can be given as follows.

$$e_a(n) = \frac{R}{(1-K_T)}[\, i^r{}_a(n) - K_T\, i^r{}_a(n-1)\,] \tag{21}$$

The solution for back EMF on β-axis can be solved as mentioned above, and if the back EMF can be given on α-β axis, the electrical position angle of rotor can be following that

$$\theta_e = \tan^{-1}\frac{e_\alpha}{e_\beta}\,. \tag{22}$$

The equation obtained from Equation 22, strictly speaking, is also equal to that which passed through high-pass filter. Hence, a simple prediction method is used to remove appropriately the noise component of electrical position angle, and its schematic diagram can be illustrated in Fig. 5, where Z^{-1} means the delay term.

The block diagram of Fig. 5 can be numerically expressed as follows, where $\theta_p(K+1)$ means the prediction

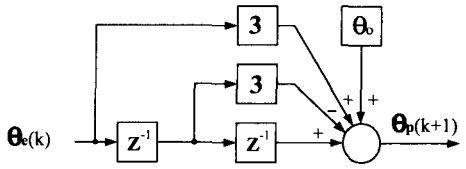

Fig. 5 Schematic diagram of quadratic position prediction

value from position angle computed by back EMF to the position angle in the next sampling, where θo means an initial position angle at a start.

$$\theta_p(k+1) = 3[\,\theta_e(k) - \theta_e(k-1)\,] + \theta_e(k-2) + \theta_o \tag{23}$$

The estimate of rotor position angle can be estimated in this method without reference to a back EMF constant, but the back EMF constant is needed to estimate the motor speed. If the given back EMF on α-β axis, the electrical angular velocity of rotor can be given as follows.

$$\omega_e = \frac{1}{K_E}\sqrt{e_\alpha^2 + e_\beta^2} \tag{24}$$

, where K_E stands for the back EMF constant. The information on the number of motor poles is necessary to find mechanical angular velocity from electrical angular velocity. The relation of electrical and mechanical angle according to the number of motor pole can be given as follows.

$$\omega_r = \frac{\omega_e}{p_{poles}} \tag{25}$$

, where p_{poles} means the motor pole pair.

2.4 The Structure of Controller

If transformed from 3-phase fixed coordinates to 2-phase fixed coordinates(α-β) in controlling PMSM, and then the latter transformed into 2-phase rotary coordinates(d-q), all values of variables come to be DC, and also their characteristic to be the same form of DC motor, which makes a control simple. The transformation and inverse transformation from 3-phase fixed coordinates to 2-phase fixed coordinates (α-β) are following that

$$\begin{bmatrix} f_q^s \\ f_d^s \\ f_o^s \end{bmatrix} = \frac{2}{3}\begin{bmatrix} 0 & \frac{\sqrt{3}}{2} & -\frac{\sqrt{3}}{2} \\ 1 & -\frac{1}{2} & -\frac{1}{2} \\ \frac{1}{2} & \frac{1}{2} & \frac{1}{2} \end{bmatrix}\begin{bmatrix} f_q \\ f_d \\ f_o \end{bmatrix} \quad (26)$$

$$\begin{bmatrix} f_q^s \\ f_d^s \end{bmatrix} = \begin{bmatrix} 0 & \frac{1}{\sqrt{3}} & -\frac{1}{\sqrt{3}} \\ \frac{2}{3} & -\frac{1}{3} & -\frac{1}{3} \end{bmatrix}\begin{bmatrix} f_q \\ f_d \\ f_o \end{bmatrix} \quad (27)$$

The transformation and inverse transformation from 2-phase fixed coordinates to 2-phase rotary coordinates (d-q) are following that

$$\begin{bmatrix} f_q^r \\ f_d^r \end{bmatrix} = \begin{bmatrix} \cos\theta & -\sin\theta \\ \sin\theta & \cos\theta \end{bmatrix}\begin{bmatrix} f_q^s \\ f_d^s \end{bmatrix} \quad (28)$$

$$\begin{bmatrix} f_q^s \\ f_d^s \end{bmatrix} = \begin{bmatrix} \cos\theta & \sin\theta \\ -\sin\theta & \cos\theta \end{bmatrix}\begin{bmatrix} f_q^r \\ f_d^r \end{bmatrix} \quad (29)$$

Fig. 6 shows the overall block diagram of proposed algorithm. The motor drive SVPWM (space vector pulse width modulation) in the block diagram uses VSI (voltage source inverter), and the space vector modulation technique is applied in the modulation method. Every algorithm except inverter is also constructed into software to make a hardware simple. The sampling time is 200μsec in this algorithm.

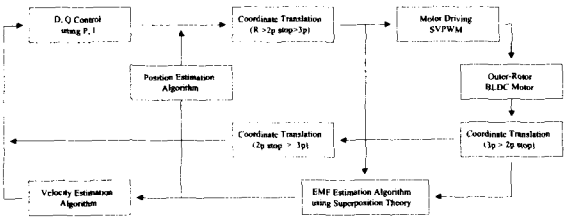

Fig. 6 Diagram of controller

There are DC-LINK voltage and phase current as inputs to realize this algorithm. After transforming the 3-phase fixed coordinates into 2-phase fixed coordinates by using these inputs, first the rotor position angle and velocity is estimated and then converted into 2-phase rotary coordinates for control.

3. Experimental Results and Analyses

3.1 The Parameter Estimation of PMSM

Fig. 7 shows PMSM which is used at experiment. As you can see in figure, Motor with 48 poles is designed for a low speed.

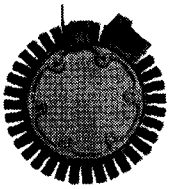

Fig. 7 PMSM at experiment

Fig. 8 shows the measured back EMF waveforms of motor, and its back EMF has good sine wave form.

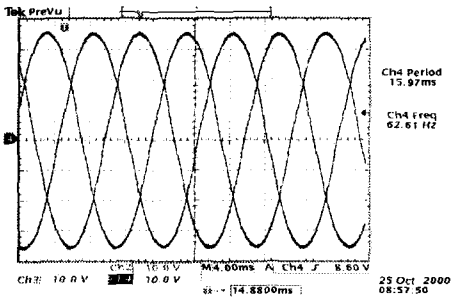

Fig. 8 back EMF waveforms of a, b, c phase

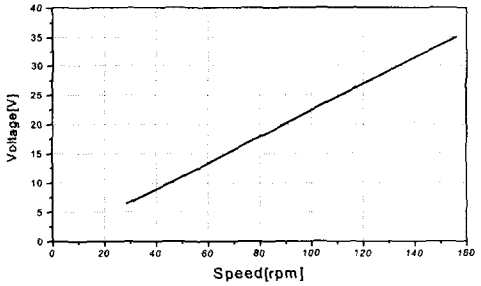

Fig. 9 back EMF of PMSM

Fig. 9 illustrates the relation between rotation speed and back EMF. It can be, like Fig. 9, found that the ratio value of back EMF to rotation speed of motor has a linearity over 98 %. Therefore, the speed can be easily solved by multiplying the back EMF constant K_E, if the back EMF is computed. When DC 24V is, moreover, forced to measure resistance R and inductance L as important parameters for sensorless control, the current waveform is shown in Fig. 10. The values of R and L can be found by analysing the rising curve of the current waveform at each phase of motor in Fig. 10.

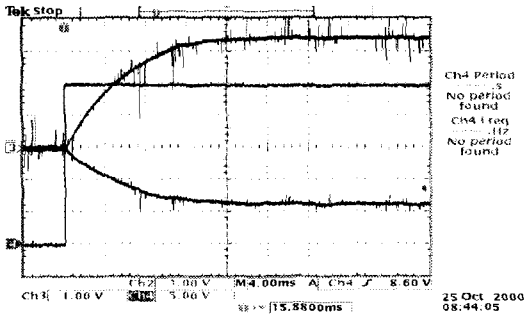

Fig. 10 Current waveform at step DC voltage

This experiments is accomplished on the magnetic field phase of PMSM with the measured parameters in Table 1.

Fig. 11 shows the waveform comparing the solution of state equation of Equation 16 with real current value by changing the terminal voltage when the back EMF is equal to zero, in order to verify measured R and L.

Table 1 The measured motor parameters

Winding resistance	1.981 [Ω]
Winding inductance	10.8 [mH]
EMF constant	0.224 [rpm/V]
Number of poles	24 [poles]
Rated current	6.0 [A]
Rated Speed	600 [rpm]

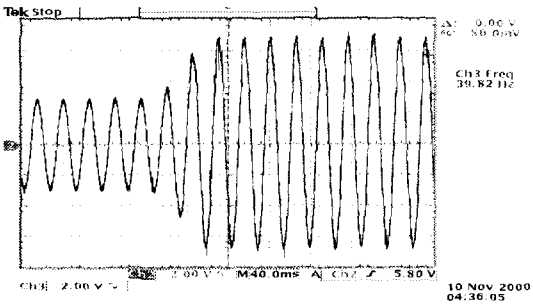

Fig. 11 Motor current and estimate current waveforms (Constrained)

In the above figure, it can be known that it estimates almost perfectly to real current with all the changes of input voltage. It shows that the measured value of R and L are accurate.

When making a short at the motor terminal, and then driving the motor with exterior power, the waveforms of the motor current and the estimate current are shown in Fig. 12. The terminal current, the estimate back EMF

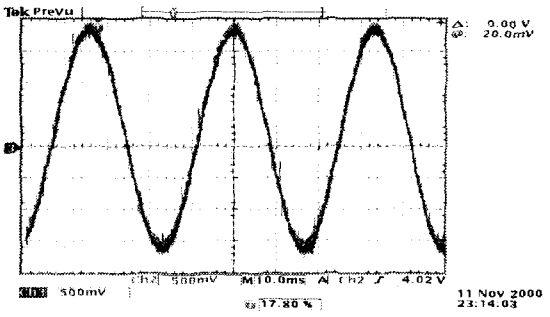

Fig. 12 Motor current and estimate current waveforms (in a short circuit)

and the electrical rotor position detected from encoder are shown in Fig. 13. As you can see in Fig. 13, it can estimate a good position because of coincidence in α -axis back EMF and the zero point of rotor.

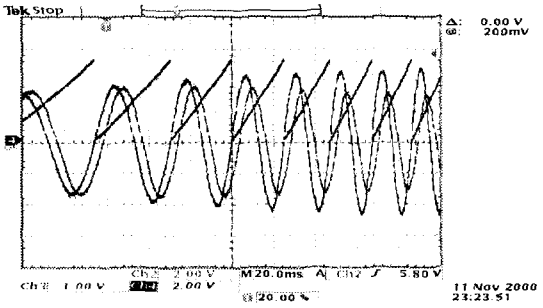

Fig. 13 Rotor current, back EMF & position of rotor

Fig. 14 shows the terminal current, the estimate current and the estimate speed in driving by the exterior motor under the same condition of Fig. 13.

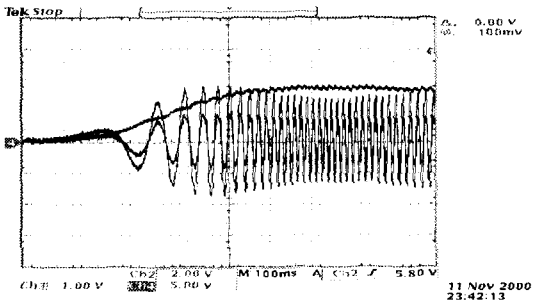

Fig. 14 Rotor current & estimate current at external start

Fig. 15 shows real rotor position and the estimate rotor position when the sensorless control is achieved

by the proposed algorithm. It can be, as you can be seen in figure, found that the estimate position of rotor is better achieved.

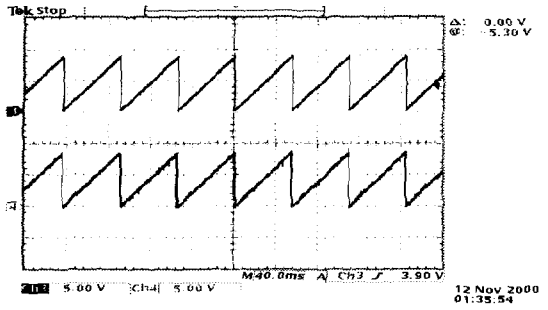

Fig. 15 Real and estimate angle

Fig. 16 shows the terminal current, the estimate angle and the real angle in driving by sensorless control. Since a cylindrical PMSM has a fixed inductance regardless of the rotor position, no information can be obtained about the initial position. Therefore, it moves with the zero initial position and then its mobile characteristic is somewhat changed by the initial position of rotor.

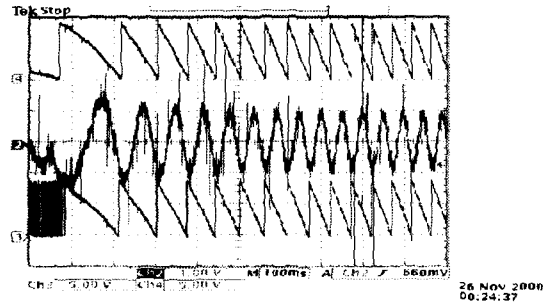

Fig. 16 Real & estimate angle at a start

4. Conclusions

In this paper, a method of sensorless control algorithm based on superposition principle is proposed. After the state equation of motor is separated into two state equations in each constraint and short circuit, they are analysed. Based on this analysis, the back EMF component can be analysed by simply computing the short circuit current by motor's back EMF component in operation, whereby a position angle computation technique is proposed. The experiment using a PMSM in a washing machine is made to verify a properness of control algorithm and then results in the following characteristics.

1. In this control algorithm, the rotor's position can be estimated without an information about back EMF constant.
2. The mobile characteristic somewhat can be changed by the initial rotor position at a start. When the rotor position is aligned to fix the initial position, the alignment characteristic can be different by the rotor position.

If this control algorithm is applied to the PMSM, an improvement in productivity and an increase on durability is expected by not only the performance improvement of products but also the simple structure. In addition, even though a motor characteristic or a manufacturing maker is changed, the changed system can be accessed by using the known motor parameters.

References

1. Jahns, T. M., "Torque production in permanent magnet synchronous motor drives with rectangular current excitation," IEEE Trans. Indust. Applicat., Vol. 20, No. 4, pp. 803-813, July/June 1984.
2. Bolton, H. R. and Ashen, R. A., "Influence of motor design and feed-current waveform on torque ripple in brushless DC drive," Proc. of IEE, Vol. 131, Part B, No. 3, pp. 82-90, May 1984.
3. Hanselman, D., Hung, J. Y. and Keshura, M., "Torque ripple analysis in brushless permanent magnet motor drive," Proc. of ICEM 92, Manchester, UK, pp. 823-827, Sept. 1992.
4. Le-Huy, H., Perret, R. and Feuillet, R., "Minimization of torque ripple in brushless DC motor drive," IEEE Trans. Indust. Applicat., Vol. 22, No. 4, pp. 748-755, July/Aug. 1986.
5. Hung, J. Y. and Ding, Z., "Minimization of torque ripple in permanent magnet motors," Proc. 18th IEEE Industrial Electronics Conf., San Diego, CA, pp. 459-463, Nov. 1992.
6. Hanselman, D., "Minimum Torque Ripple, Maximum Efficiency Excitation of Brushless Permanent Magnet Motors," IEEE Trans. Ind. Applicat., Vol. 41, No. 3, pp. 292-300, June 1994.